



**Citation:** A. Çetinbaş-Genç, C. Bayam, F. Vardar (2021) Morphological, biochemical and molecular hallmarks of programmed cell death in stigmatic papillae of *Brassica oleracea* L.. *Caryologia* 74(1): 117-126. doi: 10.36253/caryologia-1035

**Received:** July 28, 2020

**Accepted:** April 26, 2021

**Published:** July 20, 2021

**Copyright:** © 2021 A. Çetinbaş-Genç, C. Bayam, F. Vardar. This is an open access, peer-reviewed article published by Firenze University Press (<http://www.fupress.com/caryologia>) and distributed under the terms of the Creative Commons Attribution License, which permits unrestricted use, distribution, and reproduction in any medium, provided the original author and source are credited.

**Data Availability Statement:** All relevant data are within the paper and its Supporting Information files.

**Competing Interests:** The Author(s) declare(s) no conflict of interest.

**ORCID**

AÇG: 0000-0001-5125-9395

## Morphological, biochemical and molecular hallmarks of programmed cell death in stigmatic papillae of *Brassica oleracea* L.

ASLIHAN ÇETINBAŞ-GENÇ\*, CANSU BAYAM, FILİZ VARDAR

Department of Biology, Marmara University, Kadıköy, 34722, İstanbul, Turkey

\*Corresponding author. E-mail: aslihan.cetinbas@marmara.edu.tr

**Abstract.** The aim of this study is to determine the programmed cell death hallmarks in the stigmatic papillae of *Brassica oleracea* L. The flower development was divided in two main stages; pre-anthesis and post-anthesis. Programmed cell death hallmarks were examined in parallel to these stages. At pre-anthesis, the stigmatic papillae were ovoid and their dense cytoplasm were rich in insoluble polysaccharide and protein. At post-anthesis, vacuolization and enlargement were quite evident in papillae. Besides, the protein content decreased, but reactive oxygen species increased in comparison to the pre-anthesis stage. Although no significant change in superoxide dismutase activity was detected, catalase activity decreased and hydrogen peroxide content increased at post-anthesis. DAPI stained nuclei appeared rounded and smooth appearance at pre-anthesis, however, some invaginations and fragmentation in nuclei were observed at post-anthesis. Although, TUNEL staining was negative at pre-anthesis, while TUNEL positive reaction was significant in the nuclei of papillae at post-anthesis. In comparison to the pre-anthesis, the number of fragmented nuclei monitored by DAPI and TUNEL staining increased at post-anthesis.

**Keywords:** programmed cell death, papillae, reactive oxygen species, sexual plant reproduction, TUNEL.

### 1. INTRODUCTION

*Brassica oleracea* is a member of Brassicaceae family consisting of 4060 species (Bayer et al. 2019). It is an important agronomic plant due to its consumption as a vegetable (Neik et al. 2017). Flowers of *B. oleracea* have 4 sepals, 4 petals, 2 short and 4 long anthers, and one pistil (Arın 2005). Stigma is the pollen receptive surface of the pistil (Edlun et al. 2004). There are two types of stigmas in angiosperms; wet and dry type. Wet type stigmas produce stigmatic secretions while the dry typed stigmas are devoid of stigmatic secretion. In dry typed stigmas, a protein-based pellicle layer covers the papillae cuticle. Despite this distinction between wet and dry stigmas, stigmatic papillae are characterized by the expression of various biomolecules such as the various organic matters such as insoluble polysaccharide and protein, enzymes, and

reactive oxygen species (ROS) in both types. (McInnis et al. 2006). For instance, stigmatic papillae contain proteins, lipids, carbohydrates that are necessary for pollen germination (Edlund et al. 2004). Also, stigmatic enzymes are necessary for stigma receptivity and function (Souza et al. 2016). Besides, ROS regulates the stigma receptivity and plays as a signal molecule in the pollen germination process (Zafra et al. 2010). During development, the expression of these biomolecules shows various changes due to several processes such as organ aging, pollination, cell death and etc.

Programmed cell death (PCD) is a genetically regulated complex process for plant lifespan. It has been proved that PCD is a necessary process both in developmental and defense processes for plants (Serrano et al. 2010). So, it is investigated in two types; environmentally induced (ePCD) and developmentally regulated (dPCD) (van Hautegem et al. 2015). While both types are significant processes, dPCD particularly has an important function during plant life. dPCD occurs in various cells, tissues, or organs for various purposes. However, reproductive development is a rich arena as a showcase for dPCD in plants. Because dPCD can take place in sex determination, anther tapetum, megasporangium, synergid, and antipodal cells, nucellus, endosperm, stylar transmitting tissue, stigmatic papillae or etc. (Brighigna et al. 2006; Vardar and Ünal 2012; Papini et al. 2011). dPCD is accompanied by various developmental stages at stigma during female reproductive organ development. For instance, stigma no longer required for a flower after pollination and it is eliminated by PCD (Rogers 2006). The stigmatic branches of *Actinidia chinensis* are degenerated by dPCD after pollination (Ferradas et al. 2014). Also, Stigma goes PCD when incompatible pollen lands on the stigma. Thus, PCD is involved in the pollen selection process of stigma (Wu and Cheung 2000). For instance, the stigmatic papillae undergo dPCD after incompatible pollination in *Olea europaea* (Serrano et al. 2010).

Characteristic hallmarks of dPCD in plants can be observed by various morphological, biological, and molecular methods. The fundamental descriptive hallmarks are cell shrinkage, cytoplasmic and nuclear breakdown, and DNA fragmentation (Serrano et al. 2010). Also, ROS accumulation is among the hallmarks of PCD causing harmful chain effects in the cell. Since the accumulation of ROS causes oxidative stress, they are balanced by scavenging mechanisms including antioxidants such as superoxide dismutase (SOD) and catalase (CAT) (Apel and Hirt 2004; Pandhair and Sekhon 2006). SOD accelerates the conversion of superoxide, which is one of the reactive and toxic ROS, to hydrogen peroxide ( $H_2O_2$ ). CAT catalyzes the deterioration of  $H_2O_2$  thereby over-

coming oxidative stress. So, changes in SOD and CAT enzyme activity and  $H_2O_2$  content can give hint about the level of oxidative stress (Wang et al. 2010).

The aim of the present study is to investigate the morphological, biochemical, and molecular hallmarks of dPCD in stigmatic papillae of *Brassica oleracea* L. The obtained results may provide new insights into the role of dPCD in stigma development and help to improve the knowledge on dPCD hallmarks in reproductive organs. To this end, we assayed different dPCD markers in stigmatic papillae excised from flowers at pre-anthesis and post-anthesis.

## 2. MATERIAL AND METHODS

### 2.1 Determination of flower development stage

Flowers of *B. oleracea* L. were collected from the vicinity of Akçakoca/Düzce (Turkey) in 2019. The stigma development was divided into 2 main stages (pre-anthesis and post-anthesis) correlated with some morphological markers of the flower such as the position of calyx and corolla, anther dehiscence, and the absence or presence of pollen on it. The flower buds with calyx covering half of the bud and collected 2-3 days before anthesis were accepted at pre-anthesis. At this stage, there were no pollen grains on the stigma, because the anthers were still indehiscent. The flowers with senescent petals and collected 2-3 days after anthesis were accepted at post-anthesis. At this stage, a lot of pollen grains were visible on the stigma due to anther dehiscence.

### 2.2 Morphological and biochemical changes

After fixation in acetic acid:alcohol solution (1:3, v/v), pistils were dehydrated and embedded in paraffin blocks. To investigate the morphological and biochemical changes, sections (8-10  $\mu m$ ) were stained with Periodic Acid-Schiff (PAS) (Feder and O'Brien 1968) for insoluble polysaccharides and, stained with Coomassie Brilliant Blue (CBB) (Fisher 1968) for proteins. Images were captured using Olympus BX-51 microscope and KAMERAM software. The optical density (OD) of insoluble polysaccharide and protein contents of papillae were computed using Image J software (Rodrigo et al. 1997). 20 papillae were used for each group.

### 2.3 ROS accumulation and antioxidant enzyme activity

ROS accumulation of papillae was determined according to previous studies (Fabian et al. 2019). Fresh

tissues were labeled by 20  $\mu\text{M}$  2',7'-dichlorodihydro-fluorescein diacetate ( $\text{H}_2\text{DCFDA}$ ) and images were captured using Olympus BX-51 fluorescence microscope and KAMERAM software. Fluorescence intensities of 20 papillae were measured using the Image J software. Superoxide dismutase (SOD) and catalase (CAT) activities were detected according to Li et al. (2000) and Prochazkova et al. (2001), respectively. After homogenization of 0.03 g tissue in 1500  $\mu\text{l}$  50 mM PBS (pH 7.8) and centrifugation at 12,000 $\times g$  for 15 min, supernatants were used as SOD and CAT enzyme source. To measure the spectrophotometric SOD activity, 300  $\mu\text{l}$  supernatant (same volume of 50 mM PBS for control) was added to 2400  $\mu\text{l}$  measurement buffer containing 1500  $\mu\text{l}$  of 50 mM PBS (pH 7.8), 300  $\mu\text{l}$  of 130 mM L-methionine, 300  $\mu\text{l}$  of 750  $\mu\text{M}$  nitro blue tetrazolium, 300  $\mu\text{l}$  of 100  $\mu\text{M}$  EDTA-Na<sub>2</sub>. After incubation under light (50  $\mu\text{mol m}^{-2} \text{s}^{-1}$ ) for 3 minutes, SOD activity was measured at 560 nm. A non-incubated mixture was used as the blank. To measure the spectrophotometric CAT activity, 200  $\mu\text{l}$  supernatant was added to 2400  $\mu\text{l}$  measurement buffer containing 1500  $\mu\text{l}$  of 0.2 M PBS (pH 7.0) with 1% (w/v) PVP and 1000  $\mu\text{l}$  of H<sub>2</sub>O<sub>2</sub>. CAT activity was measured by the decrease in absorbance for 2 min at 240 nm. H<sub>2</sub>O<sub>2</sub> content was measured according to Junglee et al. (2014). After homogenization of 0.03 g tissue in 2000  $\mu\text{l}$  buffer containing 0.1% trichloroacetic acid, 1 M KI, 10 mM phosphate saline buffer, and centrifugation at 12,000 $\times g$  for 15 min, the supernatant was incubated in dark for 20 minutes. Afterward, H<sub>2</sub>O<sub>2</sub> content was measured at 390 nm, spectrophotometrically.

#### 2.4 Analysis of DNA Fragmentation

To determine the DNA fragmentation, 4',6-Diamidine-2'-phenylindole dihydrochloride (DAPI) (Schweizer 1976) and terminal deoxynucleotidyl transferase dUTP nick end labeling (TUNEL) (O'Brien et al. 1997) test were performed. After fixation in PBS containing 4% paraformaldehyde, pistils were dehydrated and embedded in paraffin blocks. Sections (8–10  $\mu\text{m}$ ) were stained with DAPI and, TUNEL assay was conducted using the ApopTag® Plus Fluorescein *In situ* Apoptosis Detection kit (Chemicon, Temecula, CA, USA). To avoid false-positive TUNEL results, TUNEL results were evaluated considering the control slides included in the kit supplied by the company were used. Images were captured using Olympus BX-51 fluorescence microscope and KAMERAM software. To evaluate the significant differences in nuclei undergoing PCD, percentages of DAPI stained and TUNEL positive nuclei were presented counting approximately 300 nuclei for each treatment.

#### 2.5 Statistical analysis

Statistical analyses were performed by IBM SPSS 16.0 software and data were subjected to one-way analysis of variance (ANOVA) with a threshold P value of 0.05.

### 3. RESULTS

#### 3.1 Morphological and biochemical changes

The morphological and biochemical features of papillae were investigated to analyze their main differences at pre-anthesis and post-anthesis. Papillae were ovoid and tightly packed cells at pre-anthesis. They had a thin wall, small vacuole (arrows, Fig. 1c, e), and dense cytoplasm (dots, Fig. 1c, e). Papillae cells lost their tight alignment with the increase of their diameters during the development. In comparison with the pre-anthesis, the lengths of papillae were significantly increased by 84.12% at post-anthesis (Fig. 1a). Also, the widths of papillae were significantly increased by 42.31%, in comparison with the pre-anthesis (Fig. 1b). At post-anthesis, it was remarkable that the vacuole was quite enlarged and covered a large part of the cell (arrows, Fig. 1d, f). Moreover, organic matter contents of papillae such as insoluble polysaccharide and protein were changed at post-anthesis (Fig. 1c-f). Cytoplasmic content was rich in insoluble polysaccharide and protein contents at pre-anthesis stage (Fig. 1c, e). According to the OD results of PAS stained papillae, no significant change in insoluble polysaccharide content of papillae was detected between pre-anthesis and post-anthesis (Fig. 1g). However, according to the OD results of CBB stained papillae, protein contents of papillae were significantly decreased by 33.68% at post-anthesis, when compared with the pre-anthesis (Fig. 1h).

#### 3.2 ROS accumulation and antioxidant enzyme activity

To determine the ROS accumulation difference of papillae at two development stages, stigmatic tissues were stained by  $\text{H}_2\text{DCFDA}$ . While ROS accumulation was poor at pre-anthesis, an increase in ROS accumulation was quite remarkable at post-anthesis (arrows, Fig. 2a, b). To present the subtler differences, fluorescence intensities of  $\text{H}_2\text{DCFDA}$  labeled papillae were measured. When compared with the pre-anthesis, the fluorescence intensity of  $\text{H}_2\text{DCFDA}$  was significantly increased by % 31.69 at post-anthesis (Fig. 2c). To reveal the effects of ROS accumulation on the antioxidant system, changes

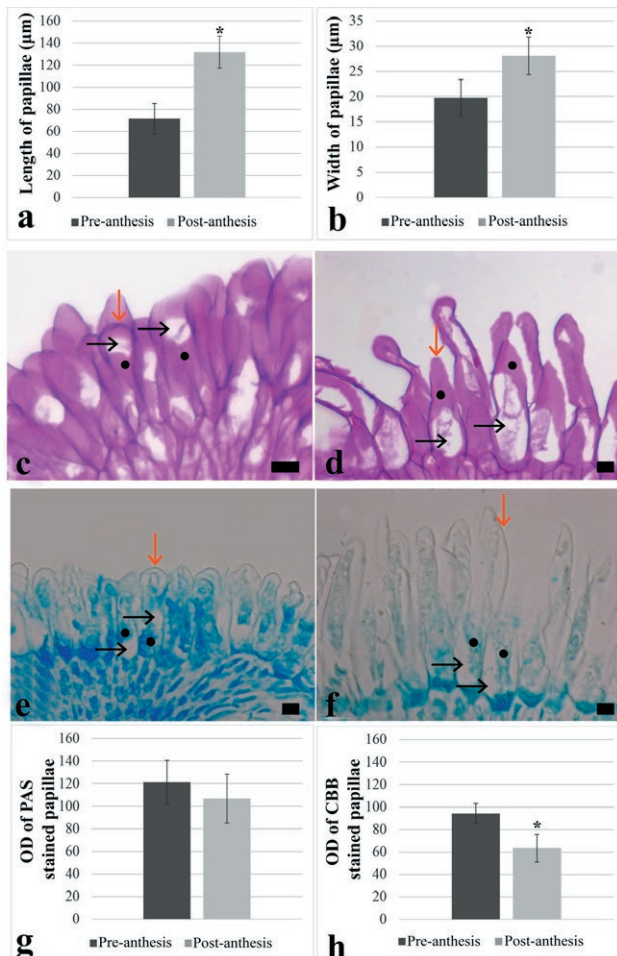


**Figure 1.** Morphological and biochemical changes of papillae at pre-anthesis and post-anthesis. **a** Length of papillae. **b** Width of papillae. **c** PAS stained papillae at pre-anthesis. **d** PAS stained papillae at post-anthesis. **e** CBB stained papillae at pre-anthesis. **f** CBB stained papillae at post-anthesis. **g** OD of PAS stained papillae. **h** OD of CBB stained papillae. Black arrows indicate the vacuoles, red arrows indicate the cell wall and points indicate the cytoplasms. Bar: 20 μm.

in SOD-CAT activity and H<sub>2</sub>O<sub>2</sub> content were investigated. When compared to pre-anthesis, no significant change in SOD activity was detected at post-anthesis (Fig. 2d). However, H<sub>2</sub>O<sub>2</sub> content was significantly increased by %23.21 (Fig. 2e) and CAT activity was significantly decreased by %37.5, at post-anthesis (Fig. 2f).

### 3.3 Analysis of Nuclear DNA Fragmentation

To determinate the nuclear morphology and DNA fragmentation, DAPI staining and TUNEL tests were performed. DAPI stained nuclei were showed rounded

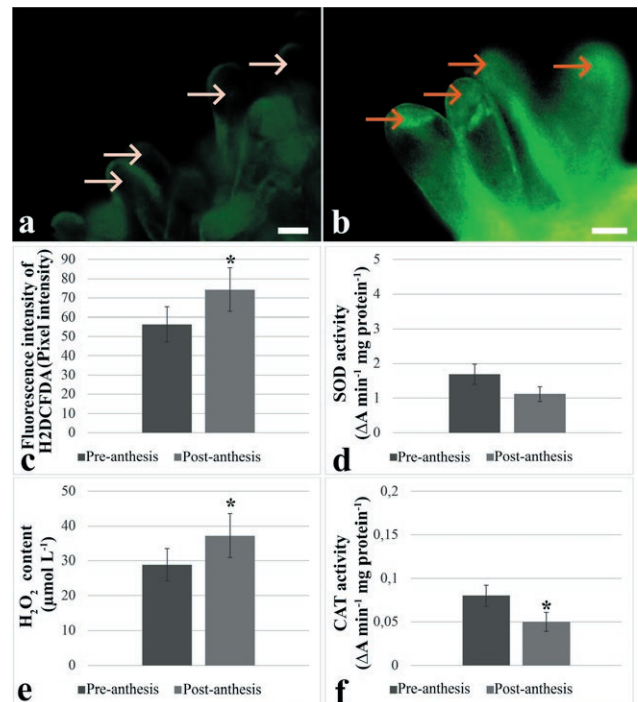


**Figure 2.** ROS accumulation and antioxidant enzyme activity of papillae at pre-anthesis and post-anthesis. **a** ROS accumulation at pre-anthesis. **b** ROS accumulation at post-anthesis. **c** Fluorescence intensity of H<sub>2</sub>DCFDA at pre-anthesis and post-anthesis. **d** Change in SOD activity. **e** Change in H<sub>2</sub>O<sub>2</sub> content. **f** Change in CAT activity. White arrows indicate the low ROS accumulation and red arrows indicate the high ROS accumulation. Bar: 20 μm.

and smooth appearance at pre-anthesis. The spherical nuclei of papillae emitted bright blue fluorescence and the chromatin was dispersed regularly (arrows, Fig. 3a). However, nuclei lost their rounded appearance and some invaginations and fragmentation were observed at post-anthesis (arrows, Fig. 3b). In comparison with the pre-anthesis, the number of fragmented nuclei monitored by DAPI staining was significantly increased about 11-fold at post-anthesis (Fig. 3e). TUNEL assay results were in parallel with the DAPI results. Although TUNEL staining was negative at pre-anthesis, the TUNEL positive reaction was significant in the nuclei of papillae at post-anthesis (arrows, Fig. 3c, d). The number of fragmented nuclei monitored by TUNEL staining was significantly increased about 6-fold at post-anthesis (Fig. 3f).

## 4. DISCUSSION

dPCD is a major process during reproductive development in plants and occurs at various developmental stages (Wang et al. 2020). Atrophy of tapetum, non-

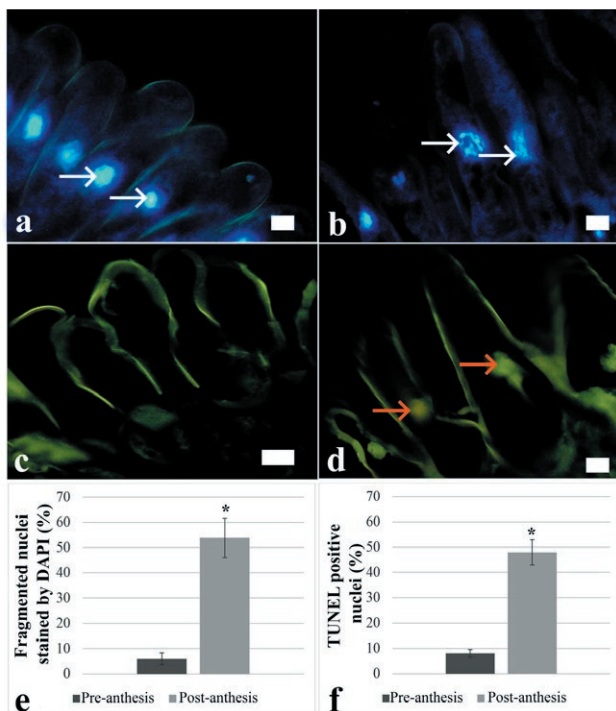


**Figure 3.** Analysis of nuclear DNA fragmentation. **a** DAPI stained spherical nuclei at pre-anthesis. **b** DAPI stained degenerated nuclei at post-anthesis. **c** TUNEL negative reaction at pre-anthesis. **d** TUNEL positive reaction at post-anthesis. **e** DAPI stained fragmented nuclei rate. **f** TUNEL positive nuclei rate. White arrows indicate the nuclear morphology and red arrows indicate the TUNEL positive nuclei. Bar: 20  $\mu$ m.

functional megasporangia, nucellus, synergids, antipodal, and suspensor cells are some examples of dPCD in the development of reproductive organs (Kurusu and Kuchitsu et al. 2017; Buono et al. 2019). Also, dPCD may take place at stigmatic branches or stigmatic papillae during female reproductive organ development. Especially papilla cell death is a good model for studying on PCD process (Ye et al. 2020). Serrano et al. (2010) have been reported that stigmatic papillae degenerated by dPCD after the pollination process in *Olea europaea*. Ferradas et al. (2014) have been described stigmatic branches of *Actinidia chinensis* degenerated after pollination. Besides, Huang et al. (2020) have been reported the PCD in stigmatic papillae of *Raphanus sativus* and *Brassica napa* after pollination. According to our results, stigmatic papillae degenerated by dPCD after the anthesis stage. Balk and Leaver (2001) have been indicated the alterations in tapetal cell morphology of *Helianthus annuus*, during dPCD. Also, Qiu et al. (2008) have been reported structural disintegration in non-functional megasporangia of *Lactuca sativa* during dPCD. Serrano et al. (2010) have been reported the plasma membrane

damage and alterations of cell morphology in stigmatic papillae during PCD. Also, Ferradas et al. (2014) have been indicated the progressive vacuolization and organelle disintegration in stigmatic branches during PCD. Similarly, we detected some alterations in the shapes of papillae cells at post-anthesis. These alterations were probably related to both the increase of their diameters and dPCD process.

During dPCD processes, researchers have been reported the vacuolization in the inner integument of *Brassica napus* (Wan et al. 2002), in tapetal cells of *Oryza sativa* (Ku et al. 2003) and in tapetum and filament of *Lathyrus undulatus* (Vardar and Ünal 2012). Besides, vacuolization was reported during dPCD processes of style tissue of *Ficus carica* (Aytürk and Ünal 2018), stigma of *Arabidopsis thaliana* (Gao et al. 2018), and anther and ovule of *Opuntia robusta* (HernandezCruz et al. 2019). Parallel to these literatures, it was remarkable that the vacuoles were large and covered the large part of the cell at the post-anthesis stage which we detected the dPCD. Researchers have been reported the decrease in the protein content of cytoplasm in petals of *Nicotiana tabacum* (Serafini-Fracassini et al. 2002), in tepals of *Iris* and *Alstroemeria* (Wagstaff et al. 2005) and *Lilium candidum* (Mochizuki-Kawai et al. 2015) during dPCD. Similar to these findings, we detected the decrease in the protein content of papillae at the post-anthesis stage which we detected the dPCD.

ROS is the major regulator of plant growth and development due to its interaction capability with all cellular substances such as protein, lipid, signaling molecules, hormones and etc. (Waszczak et al. 2018; Sankaranarayanan et al. 2020). ROS acts as cellular signaling molecules in lower doses. However excessive ROS production leads to PCD (Oracz and Karpinsky 2016). Yadegari and Drews (2004) have been specified that ROS plays vital role in the control and implementation of dPCD of aleurone and endosperm cells. Also, Hayashi et al. (2001) have indicated that ROS accumulation in the central cell of the embryo sac acted as a signal molecule in dPCD of antipodal cells. Besides, Tripathi and Tuteja (2007) have been reported that ROS is accompanied to dPCD process in sepals, petals, and ovules. Duan et al. (2014) have been specified that ROS production caused cell wall alteration for the reception of pollen tubes in synergid cells of *Arabidopsis thaliana* by causing dPCD in them. Also, van Durme and Nowack (2016) have been implicated that ROS signal regulates the dPCD of tapetal cells at the right time. ROS also has a role in signaling networks promoting pollen germination and pollen tube growth on stigma. Thus, the concentration of ROS on the stigma affects the stigma receptivity and germination.

nation capability of pollen (Zafra et al. 2010). Breygina et al. (2020) and Zhang et al. (2020) have been reported that proper doses of ROS in stigma exudate are important for the communication between the pollen/pollen tube and female tissues at various stages. However, excessive ROS accumulation may induce the dPCD of papillae. Researchers have been reported ROS-mediated dPCD occurred in papillae during incompatible pollination in the *Olea europaea* (Serrano et al. 2015). According to our results, the intense ROS signal was quite remarkable in papillae cells at the post-anthesis stage that we detected the dPCD. One of the most commonly occurring and most stable ROS is H<sub>2</sub>O<sub>2</sub>. It generated by the reduction of superoxide anions via SOD. Also, CAT breakdown H<sub>2</sub>O<sub>2</sub> to H<sub>2</sub>O and O<sub>2</sub> (Yanık et al. 2018). Enzymes such as SOD and CAT that regulate the H<sub>2</sub>O<sub>2</sub> content show differential expression during dPCD (Singh et al. 2016). According to our results, no significant change in SOD activity was detected at post-anthesis when compared to pre-anthesis. However, H<sub>2</sub>O<sub>2</sub> content was significantly increased at post-anthesis. Also, CAT activity was significantly decreased at post-anthesis. Researchers have been reported that the high H<sub>2</sub>O<sub>2</sub> content of stigmatic papillae may be related to the stigmatic receptivity or dPCD process (Serrano et al. 2012; Xie et al. 2014). Therefore, high H<sub>2</sub>O<sub>2</sub> content in the post-anthesis indicates that the stigma is receptive at this stage. However, since dPCD occurs in papillae at post-anthesis, high H<sub>2</sub>O<sub>2</sub> content is more likely to be related to PCD. Besides, researchers have been indicated that high H<sub>2</sub>O<sub>2</sub> content is involved dPCD process of petal and tapetal cells (Tripathi and Tuteja 2007; Xie et al. 2014). Also, researchers have been reported that ROS increased due to the increased SOD and decreased CAT activities in sepals of daylily that undergoing dPCD (Panavas and Rubinstein 1998).

DAPI staining is one of the most commonly used methods for check the nuclei morphology. Researchers have been reported the various alterations by DAPI staining in chromatin, DNA, and nucleus during dPCD; such as nuclei shrinkage and chromatin condensation in tapetal cells of *Lobivia rauschii* and *Tillandsia albida* (Papini et al. 1999), chromosomal degradation in suspensor and endosperm of *Vicia faba* (Wredle et al. 2001) and, nuclear deformation and volume changes in synergid and antipodal nuclei of *T. aestivum* (An and You 2004). Also, researchers have been reported the nucleus and DNA degradation in suspensor and endosperm of *Phaseolus coccineus* (Lombardi et al. 2007), nucleus degeneration and chromatin fragmentation in synergids of *Malus domestica* (Tagliasacchi et al. 2007) and, chromatin condensation in non-functional

megaspores of *Lactuca sativa* (Qiu et al. 2008) during dPCD. Besides, nucleus and chromatin deformations in anther wall cells of *Lathyrus undulatus* (Vardar and Ünal 2012) and, chromatin condensation in stamen primordia of *Cucumis sativus* (Pawelkowicz et al. 2019) were indicated as doped hallmarks by various researchers. Also, Shi et al. (2020) have been reported chromatin fragmentation in suspensor cells undergoing PCD of *Nicotiana tabacum*. In parallel to these literatures, we detected the various invaginations and fragmentation in papillae nuclei at the post-anthesis stage which we detected the dPCD. Similarly, Ferradas et al. (2014) have been reported that dPCD occurs in stigmatic branches and papillae of *Actinidia chinensis* after pollination, and chromatin condensation and nucleus degradation are quite remarkable during this dPCD process. Besides, Gao et al. (2018) have been shown the nucleus degradation in stigmatic papillae of *Arabidopsis thaliana* during dPCD. Also, TUNEL method is one of the most common and definitive methods used to determine PCD. It allows the determine PCD by marking the free 3'OH ends of DNA formed by endonucleases in cells. Researchers have been detected the TUNEL positive reaction in cells undergoing PCD such as in filament of *Hordeum vulgare* (Wang et al. 1999), in tapetal cells of *Zea mays* (González-Sánchez et al. 2004) and, in suspensor and endosperm of *Phaseolus coccineus* (Lombardi et al. 2007). Also, TUNEL positive nuclei were detected in anther wall cells and filament of *Lathyrus undulatus* (Vardar and Ünal 2012), in style of *Ficus carica* (Aytürk and Ünal 2018), in anther of *Opuntia robusta*'s female flower (Hernández-Cruz et al. 2019) and in stamen primordia of *Cucumis sativus*'s female flower (Pawelkowicz et al. 2019). Shi et al. (2020) have been reported TUNEL positive reaction in suspensor undergoing PCD of *Nicotiana tabacum*. Jimenez-Duran et al. (2021) have been detected DNA fragmentation by TUNEL assay during the dPCD process of *Marathrum schiedeanum*'s central cell. At the post-anthesis stage, we also detected the TUNEL positive nuclei in papillae. Similarly, Ferradas et al. (2014) have been detected TUNEL positive nuclei in *Actinidia chinensis*'s stigmatic branches and papillae undergoing dPCD. Also, Gao et al. (2018) have been reported the TUNEL positive nuclei in *Arabidopsis thaliana*'s stigmatic papillae undergoing dPCD.

## 5. CONCLUSION

In conclusion, our results including vacuolization, decreased protein content, increased ROS content, increased H<sub>2</sub>O<sub>2</sub> content and decreased CAT activ-

ity, and also nuclear fragmentation marked by DAPI and TUNEL positive nuclei at the post-anthesis stage revealed that papillae cells undergo dPCD at the post-anthesis stage. We think that our results will contribute to a clear understanding of dPCD in plants, especially during reproductive development.

#### ACKNOWLEDGEMENTS

We thank Prof Meral Ünal for her support. This research did not receive any specific grant from funding agencies in the public, commercial, or not-for-profit sectors.

#### REFERENCES

- An LH, You RL (2004) Studies on nuclear degeneration during programmed cell death of synergid and antipodal cells in *Triticum aestivum*. *Sex Plant Reprod* 17(4):195-201. <https://doi.org/10.1007/s00497-004-0220-1>
- Apel K, Hirt H (2004) Reactive oxygen species: metabolism, oxidative stress, and signal transduction. *Annu Rev Plant Biol* 55:373-399. <https://doi.org/10.1146/annurev.arplant.55.031903.141701>
- Arın L (2005) Alabaş (*Brassica oleraceae* var. *gongylodes* L.) Yetişiriciliği. *Alatarım* 4(2):13-17.
- Aytürk Ö, Ünal M (2018) Reorganization of microtubules in pistil cells undergoing programmed cell death in *Ficus carica* L. *Caryologia* 71(4):482-488. <https://doi.org/10.1080/00087114.2018.1505238>
- Balk J, Leaver CJ (2001) The PET1-CMS mitochondrial mutation in sunflower is associated with premature programmed cell death and cytochrome c release. *The Plant Cell* 13(8):1803-1818. <https://doi.org/10.1105/TPC.010116>
- Bayer PE, Golicz AA, Tirnaz S, Chan CKK, Edwards D, Batley J (2019) Variation in abundance of predicted resistance genes in the *Brassica oleracea* pan-genome. *Plant Biotech J* 17(4):789-800. <https://doi.org/10.1111/pbi.13015>
- Buono RA, Hudecek R, Nowack MK (2019) Plant proteases during developmental programmed cell death. *J Exp Bot* 70(7):2097-2112. <https://doi.org/10.1093/jxb/erz072>
- Breygina M, Klimentko E, Shilov E, Mamaeva A, Zgoda V, Fesenko I (2020) ROS in tobacco stigma exudate affect pollen proteome and provoke membrane hyperpolarization. *bioRxiv*. <https://doi.org/10.1101/2020.04.28.065706>
- Brighigna L, Papini A, Milocani E, Vesprini JL (2006) Programmed cell death in the nucellus of *Tillandsia* (Bromeliaceae). *Caryologia* 59(4):334-339. <https://doi.org/10.1080/00087114.2006.10797935>
- Duan Q, Kita D, Johnson EA, Aggarwal M, Gates L, Wu HM, Cheung AY (2014) Reactive oxygen species mediate pollen tube rupture to release sperm for fertilization in *Arabidopsis*. *Nat Commun* 5:3129. <https://doi.org/10.1038/ncomms4129>
- Edlund AF, Swanson R, Preuss D (2004) Pollen and stigma structure and function: the role of diversity in pollination. *The Plant Cell* 6(suppl 1):S4-S97. <https://doi.org/10.1105/tpc.015800>
- Fabian A, Safran E, Szabo-Eitel G, Barnabas B, Jager K (2019) Stigma functionality and fertility are reduced by heat and drought co-stress in wheat. *Front Plant Sci* 10:244. <https://doi.org/10.3389/fpls.2019.00244>
- Feder N, O'Brien TP (1968) Plant microtechnique: Some principles and new methods. *Am J Bot* 55(1):123-142. <https://doi.org/10.1002/j.1537-2197.1968.tb06952.x>
- Ferradas Y, Lopez M, Rey M, Gonzalez MV (2014) Programmed cell death in kiwifruit stigmatic arms and its relationship to the effective pollination period and the progamic phase. *Ann Bot* 114(1):35-45. <https://doi.org/10.1093/aob/mcu073>
- Fisher DB, Jensen WA, Ashton ME (1968) Histochemical studies of pollen: Storage pockets in the endoplasmic reticulum. *Histochemistry* 13(2):169-182. <https://doi.org/10.1007/BF00266578>
- Gao Z, Daneva A, Salanenka Y, Van Durme M, Huysmans M, Lin Z, Winter FD, Vanneste S, Karimi M, Van de Velde J, Vandepoele K, Van de Walle D, Dewettinck K, Lambrecht BN, Nowack MK (2018) KIRA1 and ORESARA1 terminate flower receptivity by promoting cell death in the stigma of *Arabidopsis*. *Nat Plant* 4(6):365. <https://doi.org/10.1038/s41477-018-0160-7>
- Gonzalez-Sanchez M, Rosato M, Chiavarino M, Puertas MJ (2004) Chromosome instabilities and programmed cell death in tapetal cells of maize with B chromosomes and effects on pollen viability. *Genetics* 166(2):999-1009. <https://doi.org/10.1534/genetics.166.2.999>
- Hayashi Y, Yamada K, Shimada T, Matsushima R, Nishizawa NK, Nishimura MA (2001) Proteinase-storing body that prepares for cell death or stresses in the epidermal cells of *Arabidopsis*. *Plant Cell Physiol* 42:894-899. <https://doi.org/10.1093/pcp/pce144>
- Hernández-Cruz R, Silva-Martínez J, García-Campsano F, Cruz-García F, Orozco-Arroyo G, Alfaro I, Vázquez-Santana S (2019) Comparative development

- of staminate and pistillate flowers in the dioecious cactus *Opuntia robusta*. Plant Reprod 1-17. <https://doi.org/10.1007/s00497-019-00365-w>
- Jimenez-Duran K, Perez-Pacheco MK, Wong R, Collazo-Ortega M, Marquez-Guzman J (2021) Programmed cell death is the cause of central cell degeneration and single fertilization in *Marathrum schiedeanum* (Cham.) Tul (Podostemaceae). Aquat Bot 169: 103345. <https://doi.org/10.1016/j.aquabot.2020.103345>
- Junglee S, Urban L, Sallanon H, Lopez-Lauri F (2014) Optimized assay for hydrogen peroxide determination in plant tissue using potassium iodide. Am J Anal Chem 5:730–736. <https://doi.org/10.4236/ajac.2014.511081>
- Ku S, Yoon H, Suh HS, Chung YY (2003) Male-sterility of thermosensitive genic male-sterile rice is associated with premature programmed cell death of the tapetum. Planta 217(4):559–565. <https://doi.org/10.1007/s00425-003-1030-7>
- Kurusu T, Kuchitsu K (2017) Autophagy, programmed cell death and reactive oxygen species in sexual reproduction in plants. J Plant Res 130(3):491–499. <https://doi.org/10.1007/s10265-017-0934-4>
- Li HS, Sun Q, Zhao SJ, Zhang WH (2000) Experiment principle and technology of plant physiology and biochemistry. Higher Education Press, Beijing.
- Lombardi L, Ceccarelli N, Picciarelli P, Lorenzi R (2007) DNA degradation during programmed cell death in *Phaseolus coccineus* suspensor. Plant Physiol Bioch 45(3-4):221–227. <https://doi.org/10.1016/j.plaphy.2007.01.014>
- McInnis SM, Desikan R, Hancock JT, Hiscock SJ (2006) Production of reactive oxygen species and reactive nitrogen species by angiosperm stigmas and pollen: potential signalling crosstalk?. New Phytol 172(2):221–228. <https://doi.org/10.1111/j.1469-8137.2006.01875.x>
- Mochizuki-Kawai H, Niki T, Shibuya K, Ichimura K (2015) Programmed cell death progresses differentially in epidermal and mesophyll cells of lily petals. PloS one 10(11):e0143502. <https://doi.org/10.1371/journal.pone.0143502>
- Neik TX, Barbetti MJ, Batley J (2017) Current status and challenges in identifying disease resistance genes in *Brassica napus*. Front Plant Sci 8:1788. <https://doi.org/10.3389/fpls.2017.01788>
- O'Brien IE, Reutelingsperger CP, Holdaway KM (1997) Annexin-V and TUNEL use in monitoring the progression of apoptosis in plants. Cytometry 29(1):28–33. [https://doi.org/10.1002/\(SICI\)1097-0320\(19970901\)29:1<28::AID-CYTO2>3.0.CO;2-9](https://doi.org/10.1002/(SICI)1097-0320(19970901)29:1<28::AID-CYTO2>3.0.CO;2-9)
- Oracz K, Karpinski S (2016) Phytohormones signaling pathways and ROS involvement in seed germination. Front Plant Sci 7:864. <https://doi.org/10.3389/fpls.2016.00864>
- Panavas T, Rubinstein B (1998) Oxidative events during programmed cell death of daylily (*Hemerocallis hybrid*) petals. Plant Sci 133(2):125–138. [https://doi.org/10.1016/S0168-9452\(98\)00034-X](https://doi.org/10.1016/S0168-9452(98)00034-X)
- Pandhair V, Sekhon BS (2006) Reactive oxygen species and antioxidants in plants: an overview. J Plant Biochem Biot 15(2):71–78. <https://doi.org/10.1007/BF03321907>
- Papini A, Mosti S, Brighigna L (1999) Programmed-cell-death events during tapetum development of angiosperms. Protoplasma 207(3-4):213–221. <https://doi.org/10.1007/BF01283002>
- Papini A, Mosti S, Milocani E, Tani G, Di Falco P, Brighigna L (2011) Megasporogenesis and programmed cell death in *Tillandsia* (Bromeliaceae). Protoplasma 248(4):651–662. <https://doi.org/10.1007/s00709-010-0221-x>
- Pawelkowicz ME, Skarzynska A, Plader W, Przybecki Z (2019) Genetic and molecular bases of cucumber (*Cucumis sativus* L.) sex determination. Mol Breeding 39(3):50. <https://doi.org/10.1007/s11032-019-0959-6>
- Prochazkova D, Sairam RK, Srivastava GC, Singh DV (2001) Oxidative stress and antioxidant activity as the basis of senescence in maize leaves. Plant Sci 161(4):765–771. [https://doi.org/10.1016/S0168-9452\(01\)00462-9](https://doi.org/10.1016/S0168-9452(01)00462-9)
- Qiu YL, Liu RS, Xie CT, Russell SD, Tian HQ (2008) Calcium changes during megasporogenesis and mega-spore degeneration in lettuce (*Lactuca sativa* L.). Sex Plant Reprod 21(3):197–204. <https://doi.org/10.1007/s00497-008-0079-7>
- Rodrigo J, Rivas E, Herrero M (1997) Starch determination in plant tissues using a computerized image analysis system. Physiol Plant 99(1):105–110. <https://doi.org/10.1111/j.1399-3054.1997.tb03437.x>
- Rogers HJ (2006) Programmed cell death in floral organs: how and why do flowers die?. Ann Bot 97(3):309–315. <https://doi.org/10.1093/aob/mcj051>
- Sankaranarayanan, S., Ju, Y., & Kessler, S. A. (2020). Reactive Oxygen Species as Mediators of Gametophyte Development and Double Fertilization in Flowering Plants. Front Plant Sci 11:1199. <https://doi.org/10.3389/fpls.2020.01199>
- Schweizer D (1976) Reverse fluorescent chromosome banding with chromomycin and DAPI. Chromosoma 58(4):307–324. <https://doi.org/10.1007/BF00292840>
- Serafini-Fracassini D, Del Duca S, Monti F, Poli F, Sacchetti G, Bregoli AM, Biondi S, Della Mea M (2002)

- Transglutaminase activity during senescence and programmed cell death in the corolla of tobacco (*Nicotiana tabacum*) flowers. *Cell Death Diff* 9(3):309. <https://doi.org/10.1038/sj.cdd.4400954>
- Serrano I, Olmedilla A (2012) Histochemical location of key enzyme activities involved in receptivity and self-incompatibility in the olive tree (*Olea europaea* L.). *Plant Sci* 197:40–49. <https://doi.org/10.1016/j.plantsci.2012.07.007>
- Serrano I, Pellicione S, Olmedilla A (2010) Programmed-cell-death hallmarks in incompatible pollen and papillar stigma cells of *Olea europaea* L. under free pollination. *Plant Cell Rep* 29(6):561–572. <https://doi.org/10.1007/s00299-010-0845-5>
- Serrano I, Romero-Puertas MC, Sandalio LM, Olmedilla A (2015) The role of reactive oxygen species and nitric oxide in programmed cell death associated with self-incompatibility. *J Exp Bot* 66(10):2869–2876. <https://doi.org/10.1093/jxb/erv083>
- Shi C, Luo P, Zhao P, Sun MX (2020) Detection of embryonic suspensor cell death by whole-mount TUNEL assay in tobacco. *Plants* 9(9):1196. <https://doi.org/10.3390/plants9091196>
- Singh R, Singh S, Parihar P, Mishra RK, Tripathi DK, Singh VP, Chauhan DK, Prasad SM (2016) Reactive oxygen species (ROS): beneficial companions of plants' developmental processes. *Front Plant Sci* 7:1299. <https://doi.org/10.3389/fpls.2016.01299>
- Souza EH, Carmello-Guerreiro SM, Souza FVD, Rossi ML, Martinelli AP (2016) Stigma structure and receptivity in Bromeliaceae. *Sci Hort* 203:118–125. <https://doi.org/10.1016/j.scienta.2016.03.022>
- Tagliasacchi AM, Andreucci AC, Giraldi E, Felici C, Ruberti F, Forino LMC (2007) Structure, DNA content and DNA methylation of synergids during ovule development in *Malus domestica* Borkh. *Caryologia* 60(3):290–298. <https://doi.org/10.1080/00087114.2007.10797950>
- Tripathi SK, Tuteja N (2007) Integrated signaling in flower senescence: an overview. *Plant Signal Behav* 2(6):437–445. <https://doi.org/10.4161/psb.2.6.4991>
- Van Durme M, Nowack MK (2016) Mechanisms of developmentally controlled cell death in plants. *Curr Opin Plant Biol* 29:29–37. <https://doi.org/10.1016/j.pbi.2015.10.013>
- Van Hautegem T, Waters AJ, Goodrich J, Nowack MK (2015) Only in dying, life: programmed cell death during plant development. *Trends Plant Sci* 20(2):102–113. <https://doi.org/10.1016/j.tplants.2014.10.003>
- Vardar F, Ünal M (2012) Development and programmed cell death in the filament cells of *Lathyrus undulatus* Boiss. *Caryologia* 64(2):164–172. <https://doi.org/10.1080/00087114.2002.589779>
- Wagstaff C, Chanasut U, Harren FJ, Laarhoven LJ, Thomas B, Rogers HJ, Stead AD (2005) Ethylene and flower longevity in Alstroemeria: relationship between tepal senescence, abscission and ethylene biosynthesis. *J Exp Bot* 56(413):1007–1016. <https://doi.org/10.1093/jxb/eri094>
- Wan L, Xia Q, Qiu X, Selvaraj G (2002) Early stages of seed development in *Brassica napus*: a seed coat-specific cysteine proteinase associated with programmed cell death of the inner integument. *The Plant Journal* 30(1):1–10. <https://doi.org/10.1046/j.1365-313X.2002.01262.x>
- Wang M, Hoekstra S, van Bergen S, Lamers GE, Oppedijk BJ, van der Heijden MW, Priesder W, Schilperoort RA (1999) Apoptosis in developing anthers and the role of ABA in this process during androgenesis in *Hordeum vulgare* L. *Plant Mol Biol* 39(3):489–501. <https://doi.org/10.1023/A:1006198431596>
- Wang P, Du Y, Li Y, Ren D, Song CP (2010) Hydrogen peroxide-mediated activation of MAP kinase 6 modulates nitric oxide biosynthesis and signal transduction in *Arabidopsis*. *The Plant Cell* 22(9):2981–2998. <https://doi.org/10.1105/tpc.109.072959>
- Wang Y, Ye H, Bai J, Ren F (2020) The regulatory framework of developmentally programmed cell death in floral organs: A review. *Plant Physiol Biochem* 158:103–112. <https://doi.org/10.1016/j.plaphy.2020.11.052>
- Waszczak C, Carmody M, Kangasjärvi J (2018) Reactive oxygen species in plant signaling. *Annu Rev Plant Biol* 69:209–236. <https://doi.org/10.1146/annurev-arplant-042817-040322>
- Wredle U, Walles B, Hakman I (2001) DNA fragmentation and nuclear degradation during programmed cell death in the suspensor and endosperm of *Vicia faba*. *Int J Plant Sci* 162(5):1053–1063. <https://doi.org/10.1086/321922>
- Wu HM, Cheung AY (2000) Programmed cell death in plant reproduction, in: Lam, E., Fukuda, H., Greenberg, J. (Eds.), In *Programmed Cell Death in Higher Plants*, Springer, Dordrecht, pp. 23–37.
- Xie HT, Wan ZY, Li S, Zhang Y (2014) Spatiotemporal production of reactive oxygen species by NADPH oxidase is critical for tapetal programmed cell death and pollen development in *Arabidopsis*. *Plant Cell* 26:2007–2023. <https://doi.org/10.1105/tpc.114.125427>
- Yadegari R, Drews GN (2004) Female gametophyte development. *The Plant Cell*, 16(suppl 1):S133–S141. <https://doi.org/10.1105/tpc.018192>
- Yanik F, Aytürk Ö, Çetinbaş-Genç A, Vardar F (2018) Salicylic acid-induced germination, biochemical and

- developmental alterations in rye (*Secale cereale* L.).  
Acta Bot Croat 77(1):45–50. <https://doi.org/10.2478/botcro-2018-0003>
- Ye H, Ren F, Guo H, Guo L, Bai J, Wang Y (2020) Identification of key genes and transcription factors in ageing *Arabidopsis* papilla cells by transcriptome analysis. Plant Physiol Biochem 147:1-9. <https://doi.org/10.1016/j.plaphy.2019.12.008>
- Zafra A, Rodriguez-Garcia MI, Alche JD (2010) Cellular localization of ROS and NO in olive reproductive tissues during flower development. BMC Plant Biol. 10(1):36–50. <https://doi.org/10.1186/1471-2229-10-36>
- Zhang MJ, Zhang XS, Gao XQ (2020) ROS in the male-female interactions during pollination: function and regulation. Front Plant Sci 11: 177. <https://doi.org/10.3389/fpls.2020.00177>